Supplemental Document

Optics EXPRESS

Off-axis aberrations improve the resolution limits of incoherent imaging: supplement

KEVIN LIANG[1,2,*]

[1]*Physics Department, Adelphi University, Garden City, NY 11530, USA*
[2]*The Institute of Optics, University of Rochester, Rochester NY 14627, USA*
[*]*kliang@adelphi.edu*

Supplement DOI: https://doi.org/10.6084/m9.figshare.22186894

Parent Article DOI: https://doi.org/10.1364/OE.479799

Off-axis Aberrations Improve the Resolution Limits of Incoherent Imaging: Supplement 1

Kevin Liang[1,2,*]

[1] *Physics Department, Adelphi University, Garden City, NY 11530, USA*
[2] *The Institute of Optics, University of Rochester, Rochester NY 14627, USA*
[*] *kliang@adelphi.edu*

Abstract: This document provides supplementary material for "Off-axis Aberrations Improve the Resolution Limits of Incoherent Imaging".

S1. Point spread function for shift-variant systems

In this section, a derivation via Fourier optics is provided for the field point spread function (PSF) of an imaging system that contains off-axis aberrations. Throughout the derivation, we will not be overly concerned with overall prefactors, as the PSF is ultimately normalized to ensure intensity-normalization at the image plane. Starting with a Dirac delta impulse at the object plane located at $\xi = \xi_0$, denoted $\delta(\xi - \xi_0)$ the propagation from the object plane to the pupil plane in a $4f$-imaging system is done through a Fourier transform. That is, the pupil plane field is given by

$$\delta(\xi - \xi_0) \rightarrow \int_{-\infty}^{\infty} \delta(\xi - \xi_0) \exp\left(-\mathrm{i}k\frac{\xi u}{f}\right) \mathrm{d}\xi = \exp\left(-\mathrm{i}k\frac{\xi_0 u}{f}\right). \tag{S1}$$

Note that $k = 2\pi/\lambda$ is the wavenumber. Once at the pupil plane, there are two operations to consider. First, $U_p(u, \xi_0)$ encounters an aperture, which we model as a Gaussian with characteristic width σ_p. Second, $U_p(u, \xi_0)$ encounters a phase error (aberration) function $\Delta W(u, \xi_0)$. If ΔW depends only on the pupil-plane coordinates u, it is considered an on-axis aberration and typical examples of these include defocus, spherical aberration, and other aberrations often decomposed in terms of Zernike polynomials. If ΔW includes a dependence on ξ_0, the location of the original Dirac delta impulse, then it is considered an off-axis aberration; this is the case that is the focus of our work. To summarize, the transformation to $U_p(u, \xi_0)$ at the pupil plane is described as

$$\exp\left(-\mathrm{i}k\frac{\xi_0 u}{f}\right) \rightarrow \exp\left(-\mathrm{i}k\frac{\xi_0 u}{f}\right) \exp\left(-\frac{u^2}{4\sigma_p^2}\right) \exp\left[-\mathrm{i}k\Delta W(u, \xi_0)\right]. \tag{S2}$$

The field is now inverse Fourier transformed to arrive at the image plane, where proper normalization gives us the definition of the PSF, ψ:

$$\psi(x, \xi_0) = U_0 \int_{-\infty}^{\infty} \exp\left(-\mathrm{i}k\frac{\xi_0 u}{f}\right) \exp\left(-\frac{u^2}{4\sigma_p^2}\right) \exp\left[-\mathrm{i}k\Delta W(u, \xi_0)\right] \exp\left(\mathrm{i}k\frac{ux}{f}\right) \mathrm{d}u, \tag{S3}$$

which is the definition seen in the main body, with $\xi_0 \rightarrow \xi$. Notice that, although an off-axis ΔW gives rise to shift-variance, the imaging system is still assumed to be linear. That is, if the object field, $U_o(\xi)$, is written a superposition of Dirac delta impulses:

$$U_o(\xi) = \int_{-\infty}^{\infty} U_0(\xi_0)\delta(\xi_0 - \xi)\, \mathrm{d}\xi_0, \tag{S4}$$

then

$$U_i(x) = \int_{-\infty}^{\infty} U_o(\xi)\psi(x,\xi)\,\mathrm{d}\xi. \tag{S5}$$

S2. Quantum Fisher Information for shift-variant imaging systems

A framework for calculating the quantum Fisher Information (QFI) matrix associated with parameters to be measured from the image field of a shift-variant imaging system is provided in this section. These QFI calculations provide valuable upperbounds on the information associated with various quantities of interest (such as the separation between two point sources) when the system has off-axis aberrations. To keep the derivation general, we assume that the object scene is comprised of N partially coherent point sources with point source locations $\{x_i\}_{i=1}^{N}$. Using the image-plane normalization (IN) framework in Ref. 1, the density matrix representing the object field is

$$\rho_{\mathrm{op}} = \sum_{i,j=1}^{N} \Gamma_{ij} |\xi_i\rangle\langle\xi_j|, \tag{S6}$$

where Γ is the object-plane mutual coherence matrix and $|\xi_i\rangle$ is the position ket at ξ_i, the location of the i-th point source. In the IN normalization framework, these kets may be harmlessly represented in position space as Dirac delta impulses:

$$\langle\xi|\xi_i\rangle = \delta(\xi - \xi_i) \tag{S7}$$

The transition from the object to image planes can be captured by the blurring of each point source into the point spread function (PSF), ψ, of the imaging system. In many past analyses, imaging systems were treated as being shift-invariant and therefore the resulting image of each point source can be computed as the convolution of ψ with the Dirac delta impulse, given by Eq. (S7) of each point source. However, for shift-variant systems, one must instead consider

$$|\xi_i\rangle \longrightarrow |\psi_i\rangle, \tag{S8}$$

where

$$|\psi_i\rangle = \int_{-\infty}^{\infty} \psi(x,\xi_i)|x\rangle. \tag{S9}$$

Importantly, Eq. (S9) indicates that the PSF $\psi(x,\xi_i)$ depends on both the image-plane position coordinate, x, and the point source's object plane location, ξ_i, in a manner that may not be expressible through their difference $x - \xi_i$ alone. We are primarily interested in the case where the imaging system contains off-axis tilt (OAT) and Petzval curvature. As seen in the main body, this leads to a normalized PSF given by

$$\psi(x,\xi;P,T) = \frac{1}{[2\pi g^2(\xi;P)]^{1/4}} \exp\left\{-\frac{[x-\xi(1+2\pi T\sigma)]^2}{4g^2(\xi,P)} + \mathrm{i}\Phi(x,\xi;P,T)\right\}, \tag{S10}$$

where

$$g(\xi;P) \triangleq \sigma\sqrt{1+4\pi^2P^2\xi^4}, \tag{S11}$$

is the characteristic width of ψ and

$$\Phi(x,\xi;P,T) \triangleq -\frac{1}{2}\left\{\tan^{-1}(2\pi P\xi^2) + \frac{\pi P\xi^2[x-\xi(1+2\pi T\sigma)]^2}{g^2(\xi;P)}\right\}, \tag{S12}$$

is the phase of ψ. The values of T and P refer to the strength of OAT and Petzval, respectively (the case of $T = P = 0$ reduces the PSF to the shift-invariant, aberration free case). It's important to note that the *width* of the PSF in Eq. (S10) is such that $g \geq \sigma$, where σ is the width of the aberration-free PSF; the equality is attained when $P = 0$ (no Petzval curvature). As is done in Refs. 1 and2, it is convenient to re-express the PSF in terms by introducing the dimensionless position variable $\alpha = x/(2\sigma)$ so that the density matrix at the image plane can be written as

$$\rho_0 = \mathcal{N}_0^{-1} \sum_{i,j=1}^{N} \Gamma_{ij} |\alpha_i\rangle\langle\alpha_j| \tag{S13}$$

where

$$\langle\alpha|\alpha_i\rangle = \frac{1}{[\pi \bar{g}^2(\alpha_i;P)/2]^2} \exp\left\{ -\frac{[\alpha - \bar{h}(\alpha_i;T)]^2}{\bar{g}^2(\alpha_i;P)} \left[1 + \mathrm{i}\bar{v}(\alpha_i;P)\right] - \frac{\mathrm{i}}{2}\tan^{-1}\left[\bar{v}(\alpha_i;P)\right] \right\}. \tag{S14}$$

Notice that the parameters to be estimated have transformed from $\{\xi_i\} \to \{\alpha_i\}$, where $\alpha_i = \xi_i/(2\sigma)$. Furthermore, we have introduced the dimensionless functions

$$\bar{h}(\alpha_i;T) = \alpha_i(1 + 2\pi T\sigma), \tag{S15}$$

$$\bar{g}(\alpha_i;P) = \sqrt{1 + 64\alpha_i^4\pi^2P^2\sigma^4}, \tag{S16}$$

$$\bar{v}(\alpha_i;P) = 8\pi\alpha_i^2 P\sigma^2. \tag{S17}$$

Note that, in the aberration-free case, $\bar{h}(\alpha_i;0) = \alpha_i$, $\bar{g}(\alpha_i;0) = 1$, and $\bar{v}(\alpha_i;0) = 0$. The normalization factor $\mathcal{N}_0$ in Eq. (S13) is given by

$$\begin{aligned} \mathcal{N}_0 &= \sum_{i,j=1}^{N} \Gamma_{ij} \int_{-\infty}^{\infty} \langle\alpha|\alpha_i\rangle\langle\alpha_j|\alpha\rangle \, \mathrm{d}\alpha, \\ &= \sqrt{\frac{2\bar{g}_i\bar{g}_j}{\bar{g}_i^2(1+\mathrm{i}\bar{v}_j) + \bar{g}_j^2(1-\mathrm{i}\bar{v}_i)}} \exp\left[-\frac{(\bar{h}_i - \bar{h}_j)^2(\mathrm{i}+\bar{v}_i)(1+\mathrm{i}\bar{v}_j)}{\bar{g}_i^2(\mathrm{i}-\bar{v}_j) + \bar{g}_j^2(\mathrm{i}+\bar{v}_i)} \right], \end{aligned} \tag{S18}$$

where we have introduced the shorthand $\bar{h}_i, \bar{g}_i$, and $\bar{v}_i$ to for Eqs. (S15), (S16), and (S17), respectively. It's worth emphasizing that the states in Eq. (S13) are not simply coherent states with fixed widths that are shifted to location α_i. Instead, the centroid of the Gaussian and the width of the Gaussian are determined by the functions $\bar{h}$ and $\bar{g}$, respectively which *depend* on object location α_i. Such states are related to squeezed coherent states, where the centroid and widths of the Gaussian profile are fully correlated. The presence of such states in the expression for ρ_0 is a marked difference between systems that are shift-variant and the oft-studied aberration-free case.

It is also worth mentioning that the expression in Eq. (S14) can be used to represent the PSF of any system whose response to a point source located at α_i is a Gaussian centered at some location $\bar{h}(\alpha_i)$ with width $\bar{g}(\alpha_i)$. Although explicit functions for $\bar{h}$ and $\bar{g}$ are provided in the present analysis in Eqs. (S15) and (S16) for the case of OAT and Petzval curvature, the following derivation for the QFI matrix can be straightforwardly adapted for any differentiable $\bar{h}$ and $\bar{g}$. Finally, the function $\bar{v}(\alpha_i;P)$ defined in Eq. (S17) encapsulates the phasor portion of $|\alpha_i\rangle$. Although we keep our derivation general for an arbitrary mutual coherence matrix Γ, it is worth noting here that the final term within the curly braces in Eq. (S14) is irrelevant for QFI calculations when the object scene is incoherent. This is because the term is independent of α (a *global* phase) and vanishes when Eq. (S13) is diagonal (incoherent object scene). However, the presence of $\bar{v}$ persists even in the incoherent case in the first term within the curly braces in Eq. (S14).

With the density matrix ρ_0 given in Eq. (S13), one can now proceed with QFI matrix calculations to obtain the precisions associated in the measurement of unknown parameters (a subset of $\{\alpha_i\}_{i=1}^{N}$). Given the complicated nature of $|\alpha_i\rangle$, we follow a general method of deriving the QFI matrix [2–4]. A summary, and key differences/observations for the present case of a shift-variant imaging system, is provided as follows. One begins by identifying a basis that can be used to represent both ρ_0 as well as $\partial_j\rho_0$, where $\partial_j \triangleq \partial/\partial\alpha_j$ is a shorthand for parametric differentiation. Upon observation of Eq. (S13), it is clear that the union of $\{|\alpha\rangle_i\}$ and $\{\partial_i|\alpha_i\rangle\}$ is sufficient. With the sufficient basis identified, we now collect its elements in a $2N$-element vector

$$\vec{A} = \begin{bmatrix} |\alpha_1\rangle & \cdots & |\alpha_N\rangle & \partial_1|\alpha_1\rangle & \cdots & \partial_N|\alpha_N\rangle \end{bmatrix} \tag{S19}$$

so that we may express ρ_0 and $\partial_i\rho_0$ as

$$\rho_0 = \vec{A}^\dagger \cdot \rho_{0,A} \cdot \vec{A}, \tag{S20}$$

$$\partial_i\rho_0 = \vec{A}^\dagger \cdot (\partial_i\rho_{0,A}) \cdot \vec{A}. \tag{S21}$$

That is, $\rho_{0,A}$ and $\partial_i\rho_{0,A}$ are the coefficient matrices for the representation of ρ_0 and $\partial_i\rho_0$ in terms of the basis states collected in $\vec{A}$. Once this is done, one defines a $(2N)\times(2N)$ matrix Υ, which is in turn defined in terms of submatrices:

$$\Upsilon \triangleq \begin{bmatrix} \Upsilon_{\alpha\alpha} & \Upsilon_{\alpha d} \\ \Upsilon_{d\alpha} & \Upsilon_{dd} \end{bmatrix} \tag{S22}$$

The elements of these $N\times N$ Grammian submatrices are given by various inner products between basis states:

$$(\Upsilon_{\alpha\alpha})_{ij} = \langle\alpha_i|\alpha_j\rangle \tag{S23}$$

$$(\Upsilon_{\alpha d})_{ij} = \langle\alpha_i|\partial_j|\alpha_j\rangle \tag{S24}$$

$$(\Upsilon_{d\alpha})_{ij} = (\Upsilon_{\alpha d}^\dagger)_{ij} \tag{S25}$$

$$(\Upsilon_{dd})_{ij} = \langle\alpha_i|\partial_i^\dagger\partial_j|\alpha_j\rangle, \tag{S26}$$

where $\partial_i^\dagger$ indicates a derivative acting on the state to the *left*. Although analytic formulas exist for these matrix elements, given the complicated and nested nature of the parameter α_i in Eq. (S14), their explicit expressions will not be stated here. The unruliness of these expressions is a marked difference between treating an shift-variant imaging system, where the PSF is given by Eq. (S14), and an aberration-free system.

The elements of the QFI matrix, Q, can then be shown to be given by

$$(Q_0)_{ij} = 2\mathrm{vecb}(\partial_i\rho_{0,A})^\dagger \cdot (\Upsilon^{-1}\odot\rho_{0,A} + \rho_{0,A}^*\odot\Upsilon^{-1})^{-1}\cdot\mathrm{vecb}(\partial_j\rho_{0,A}), \tag{S27}$$

where $\mathrm{vecb}(\cdot)$ is the block-column vectorization operator defined through the example on its action on Υ as

$$\mathrm{vecb}(\Upsilon) = \begin{bmatrix} |\Upsilon_{\alpha\alpha}) \\ |\Upsilon_{d\alpha}) \\ |\Upsilon_{\alpha d}) \\ |\Upsilon_{dd}) \end{bmatrix},$$

where $|\cdot)$ is the column vectorization operator on a matrix [1]. In other words, $\mathrm{vecb}(\cdot)$ takes a $(2N)\times(2N)$ matrix and stacks its four $N\times N$ submatrices column-wise before those submatrices themselves are vectorized to form a $4N^2$-element vector. Finally, $\odot$ is the Tracy-Singh block Kronecker product. By defining

$$\mathbb{S} \triangleq \frac{q}{\sigma}\mathcal{N}_0^{-1}\left(\Upsilon_{\alpha\alpha}^{-1}\otimes\Gamma+\Gamma^*\otimes\Upsilon_{\alpha\alpha}^{-1}\right), \tag{S28}$$

$$\mathbb{B} \triangleq \mathbb{I}\otimes\left(\Upsilon_{\alpha\alpha}^{-1}\Upsilon_{\alpha d}\right), \tag{S29}$$

$$\bar{\mathbb{B}} \triangleq \left(\Upsilon_{\alpha\alpha}^{-1}\Upsilon_{\alpha d}\right)\otimes\mathbb{I}, \tag{S30}$$

$$\mathbb{G} \triangleq \Upsilon_{dd}-\Upsilon_{d\alpha}\Upsilon_{\alpha\alpha}^{-1}\Upsilon_{\alpha d}, \tag{S31}$$

where $\otimes$ is the Kronecker product. The QFIM can in turn be expressed as

$$Q_0 = 2(\Xi+\Xi^\dagger+\Omega+\Omega^{\mathrm{T}}), \tag{S32}$$

where Ξ and Ω are matrices with elements

$$\Xi_{ij} = \frac{(K_{0,i}^*|\mathbb{S}^{-1}|K_{0,j})}{2}+(K_{0,i}^*|\mathbb{S}^{-1}\mathbb{B}|Y_{0,j})+(K_{0,i}^*|\mathbb{S}^{-1}\bar{\mathbb{B}}|Y_{0,j}^\dagger)+(Y_{0,i}^*|\mathbb{B}^{\mathrm{T}}\mathbb{S}^{-1}\bar{\mathbb{B}}|Y_{0,j}^\dagger), \tag{S33}$$

$$\Omega_{ij} = \left(Y_{0,i}^*\middle|\mathbb{B}^{\mathrm{T}}\mathbb{S}^{-1}\mathbb{B}+\left(\mathcal{N}_0^{-1}\Gamma^*\right)^{-1}\otimes\mathbb{G}\middle|Y_{0,j}\right), \tag{S34}$$

respectively. Furthermore,

$$|K_{0,i}) \triangleq \left[\partial_i(\mathcal{N}_0^{-1})|\Gamma)-\mathcal{N}_0^{-1}\alpha_i|F_i+F_i^\dagger)\right], \tag{S35}$$

$$|Y_{0,i}) \triangleq \mathcal{N}_0^{-1}|F_i), \tag{S36}$$

are N^2-dimensional column vectors and F_i is a $N\times N$ matrix whose i-th row is the i-th row of Γ and zero elsewhere. In other words,

$$(F_i)_{kl} = \delta_{ik}\Gamma_{kl}. \tag{S37}$$

Equation (S32) is the QFI matrix corresponding to the set of unknown parameters $\{\alpha_i\}$ (or any subset of it), which are the individual locations of each point source. However, it is sometimes convenient to re-parameterize the problem in terms of the relative coordinates $\{s_i\}$, with

$$s_i = 2\sigma\begin{cases}\sum_{j=1}^{N}\alpha_j/N & i=1,\\ \alpha_i-\alpha_{i-1} & i>1.\end{cases}$$

Notice that s_1 is the centroid of the point sources and $s_{i>1}$ are successive differences between point source locations. The inverse Jacobian of this coordinate transformation is given by

$$[\mathbb{J}^{-1}]_{ij} = \frac{\partial s_i}{\partial\alpha_j} = 2\sigma\left[\frac{\delta_{i1}}{N}+\delta_{ij}-\delta_{(i-1)j}\right]. \tag{S38}$$

The QFI matrix corresponding to the new parameters $\{s_i\}$, denoted Q_0', can be written, using the inverse of Eq. (S38) as

$$Q_0' = \mathbb{J}^{\mathrm{T}}Q\mathbb{J}. \tag{S39}$$

Notice that the derivation provided above is for a general partially coherent object using the image-plane normalization scheme, and is provided for completeness. However, for the direct purposes of the present work, we are interested in the specific case where the object scene consists of two ($N=2$) point sources that are equally bright and incoherent ($\Gamma_{ij}=\delta_{ij}/2$). By taking only the parameter s_1 to be unknown (the separation between the two point sources), the QFI matrix in Eq. (S39) becomes a single number corresponding to the QFI of estimating s_1: this value is the one used and plotted in the main body of this work and labeled $Q_s(s;P,T)$.

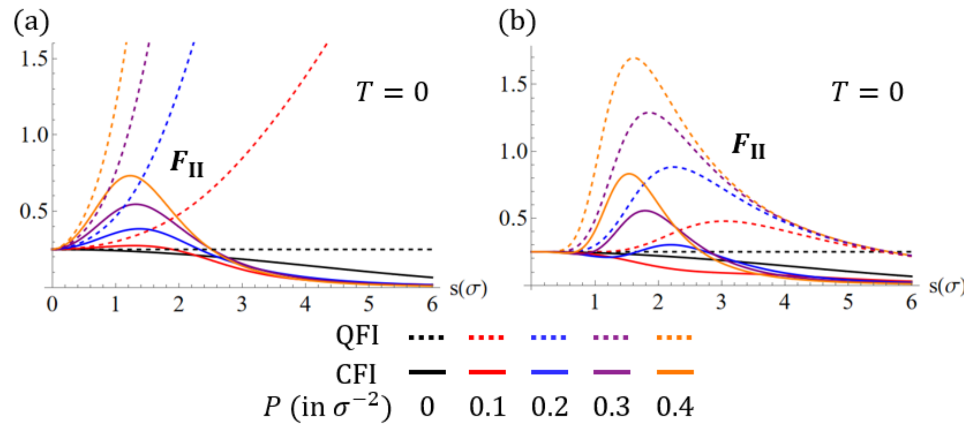

Fig. S1. QFI (dashed) and CFI (solid) are shown for imaging systems where the PSF is given by ψ (a) and $\bar{\psi}$ (b), which are given by Eqs. (S9) and (S40) respectively. There is no OAT ($T = 0$) and various values of P correspond to the different colors.

S3. Effect of the Petzval curvature phase term in PSF on QFI and CFI

The motivation of this section is to give further insight into the divergent QFI for $P \neq 0$ seen in the main body. We compare the differences in QFI and CFI for imaging systems with field PSF given by Eq. (S9) and

$$\bar{\psi}(x, \xi; P, T) = \frac{1}{[2\pi g^2(\xi; P)]^{1/4}} \exp\left\{-\frac{[x - \xi(1 + 2\pi T\sigma)]^2}{4g^2(\xi, P)}\right\}. \tag{S40}$$

It should be emphasized that Eq. (S9) is the correct PSF to be used in QFI and CFI calculations when there is Petzval curvature; however, it is worthwhile to analyze Eq. (S40) to see the effect of the phase term Φ in Eq. (S12). Before presenting the QFI results, we note that Eq. (S40) alters the probability of photon detection at the lowest order Hermite-Gauss mode as $p_{\mathrm{II}} \to \bar{p}_{\mathrm{II}}$ where

$$\bar{p}_{\mathrm{II}}(0, s; P, T) = \frac{\sqrt{1 + 4P^2\pi^2(s/2)^4}}{1 + 2P^2\pi^2(s/2)^4} \exp\left\{-\frac{(s/2)^2(1 + 2\pi T\sigma)^2}{4\sigma^2[1 + 2P^2\pi^2(s/2)^4]}\right\}. \tag{S41}$$

This leads to an altered CFI for BSPADE via $F_{\mathrm{II}} \to \bar{F}_{\mathrm{II}}$, where

$$\bar{F}_{\mathrm{II}}(s; P, T) \approx \frac{1}{\bar{p}_{\mathrm{II}}(0, s; P, T) - \bar{p}_{\mathrm{II}}^2(0, s; P, T)} \left[\frac{\partial}{\partial s}\bar{p}_{\mathrm{II}}(0, s; P, T)\right]^2. \tag{S42}$$

Figure S1(a), which also appears in the main body, shows the QFI and F_{II} for the two-point separation in an imaging system where ψ is the PSF, given by Eq. (S9). As discussed within the main body, the QFI and F_{II} coincide when $s \to 0$. However, the QFI diverges as the separation increases and is significantly different from F_{II} even within the sub-Rayleigh regime of $s < 2\sigma$. On the other hand, when the imaging system is characterized by the PSF, $\bar{\psi}$, given by Eq. (S40), Fig. S1(b) shows that the both the QFI and $\bar{F}_{\mathrm{II}}$ are comparatively smaller. In particular, the QFI no longer diverges as s increases. Therefore, the divergent behavior of the QFI for non-zero Petzval curvature is due to the presence of the phase, Φ, within the PSF, ψ. Note that Φ does not affect the CFI for direct imaging (DI) since DI is an intensity-based measurement.

References

1. K. Liang, S. A. Wadood, and A. N. Vamivakas, "Quantum fisher information for estimating n partially coherent point sources," Opt. Express **31**, 2726–2743 (2023).

2. E. Bisketzi, D. Branford, and A. Datta, "Quantum limits of localisation microscopy," New J. Phys. **21**, 123032 (1–17) (2019).
3. J. Liu, H. Yuan, X.-M. Lu, and X. Wang, "Quantum fisher information matrix and multiparameter estimation," J. Phys. A: Math. Theor. **53**, 023001 (1–68) (2019).
4. K. Liang, S. A. Wadood, and A. N. Vamivakas, "Coherence effects on estimating two-point separation," Optica **8**, 243–248 (2021).